Influences of magnetic field in Nambu-Jona-Lasinio model of three-flavor dense quark matter with axial anomaly

Xiao-bing Zhang[1], Fu-Ping Peng[1], Yun-ben Wu [1], and Yi Zhang[2]

[1]*School of Physics, Nankai University, Tianjin 300071, China and*

[2] *Department of Physics, Shanghai Normal University, Shanghai 200230, China*

(Dated: December 4, 2018)

For three-flavor and three-color quark matter, we consider coexistence of diquark and chiral condensates in the presence of magnetic fields. By incorporating magnetized color-flavor-locked matter into Nambu-Jona-Lasinio model with axial anomaly, we study influences of a rotated magnetic field on the QCD phase diagram at moderate baryon density and zero temperature. Due to its coupling to rotated-charged quarks, the magnetic field tends to facilitate a specific diquark Bose-Einstein condensation, denoted as the $\mathrm{BEC_I}$ phase. Different from the previous zero-field results, the coexistence region is superseded in favor of $\mathrm{BEC_I}$ gradually and the critical phenomena induced by axial anomaly become inhibited partially. Also, we find that an inverse catalysis of chiral phase transition happens for intermediate magnetic fields.

For stronger magnetic fields, we observe that the $\mathrm{BEC_I}$ occurrence requires smaller coupling of the chiral-diquark interplay and its location is pushed to larger quark chemical potentials. These results of $\mathrm{BEC_I}$ could have potentially importance for the physics of magnetars.

PACS numbers:

I. INTRODUCTION

Phases of quantum chromodynamics (QCD) and phase structure of strongly interacting matter have attracted great interests for years. Besides hadronic matter and quark gluon plasma, Bardeen-Cooper-Schrieffer (BCS) diquark pairing leads to quark color supercon-

ductivity at low temperature and high baryon density, see e.g. Refs. [1–3] for reviews. For three-flavor and three-color case, it corresponds to the color-flavor-locked (CFL) matter and is believed to be the ground state of QCD for sufficiently high densities [4]. The condensation of quark-antiquark pairs $\langle\bar{q}q\rangle$, namely chiral condensate, breaks chiral symmetry in the vacuum and hadronic matter. In CFL matter the condensation of diquark pairs $\langle qq\rangle$ continues to break chiral symmetry, even though $\langle\bar{q}q\rangle$ disappears at high densities. Therefore, an extensive coexistence (COE) of $\langle\bar{q}q\rangle$ and $\langle qq\rangle$ can be expected at moderate density and low temperature. In the quark matter regime there might exist the corresponding critical phenomena. This theoretical possibility was firstly pointed out in Refs. [5, 6]. By considering the QCD axial anomaly in Ginzburg-Landau framework, the interplay between chiral and diquark condensates leads to a new critical point in the phase diagram of three-flavor dense matter. Such kind of critical phenomenon was further confirmed in a Nambu-Jona-Lasinio (NJL) model with axial anomaly [7–9]. There, the chiral-diquark interplay induced by axial anomaly was introduced by six-quark effective interactions and the COE regime between a chiral-broken phase and a BCS phase of CFL matter was investigated. At moderate density and zero temperature, as detailed in Ref.[7], the critical phenomenon takes place in the sense that the Bose-Einstein condensation (BEC) of diquark "molecules" occurs firstly and then a crossover is realized from the BEC phase to an ordinary BCS phase. Different from high-temperature critical phenomena (see e.g. Ref.[10]), the above-mentioned phenomena could not be addressed with lattice QCD simulations and not be observed in experimental heavy ion programs directly.

In this paper, we discuss influences of external magnetic field on COE and possible critical phenomena at moderate density and zero temperature. The motivation for it is twofold. First of all, it is widely realized that a strong magnetic field, say the order of $eB \sim \Lambda_{QCD}^2 \sim (200\text{MeV})^2 \simeq 10^{18}\text{G}$, affects the QCD phase diagram significantly, see e.g. [11]. At low densities, it leads to that the critical chemical potential and/or critical temperature for chiral phase transition increase, i.e. the phenomenon of magnetic catalysis [12, 13]. In high-density regime where diquark condensate is dominant, a linear combination of electromagnetic and color gauge symmetries, denoted as $U(1)_{\widetilde{Q}}$, remains unbroken [4, 14]. The so-called rotated electromagnetic mechanism makes the structure of diquark condensates complicated in magnetized CFL matter. The resulting BCS phase had been extensively investigated [15–18]. Since both chiral and diquark condensates are influenced, it is theoret-

ically interesting to revisit the COE of $\langle\bar{q}q\rangle$ and $\langle qq\rangle$ and the critical phenomenon induced by axial anomaly in the presence of unscreened magnetic fields. In realistic situation, secondly, quark matter is subject to magnetic fields. The only place where color superconductivity might be observed is the astrophysical "Laboratories", e.g. the interior region of compact stars. While surface fields of magnetars have the order of 10^{14} - 10^{15}G, the magnetic field inside can reach 10^{20}G [19]. For this reason, studies of magnetized CFL matter might be important and even crucial for the physics of magnetars.

The present paper is, to our knowledge, the first to include effects of magnetic fields in the NJL description of three-flavor matter with axial-anomaly. We shall introduce an applied magnetic field B, being the rotated field corresponding to $U(1)_{\widetilde{Q}}$, and concentrate on the BEC realization of magnetized CFL matter. We do not attempt to consider the effect of confinement, which might be related with the Polyakov loop in NJL model with axial anomaly [9]. Also, we work with a simple version of three-flavor quark matter and neglect the bare quark masses, which makes the phase diagram more complicated [8]. The paper is organized as follow. After reviewing the NJL model with axial anomaly briefly, in Sec. II, we take the magnetic-induced splitting of diquark condensate into account and expand the model formalism to the situation with magnetic fields. In Sec. III, we firstly define the different BEC phases, in particular the $\mathrm{BEC_I}$ phase associated with charged relevant condensate and present the numerical results of COE phase region. Then, these results are explained in detail by the onsets of different BEC phases. Finally, we give the argument for strong fields and elucidate how $\mathrm{BEC_I}$ occurs with varying coupling of chiral-diquark interplay and quark chemical potential. We give our conclusion in Sec. IV.

II. THE NJL MODEL OF MAGNETIZED CFL MATTER WITH AXIAL ANOMALY

In this section, we firstly review the formalism of NJL model with axial anomaly given in reference[7]. And then expand it to the situation with non-vanishing magnetic fields.

ref,

A. Formalism in the absence of magnetic field

In general, the NJL-type Lagrangian reads

$$\mathcal{L} = \bar{q}(i\gamma^{\mu}\partial_{\mu} + \gamma_0\mu + m_q)q + \mathcal{L}^{(4)} + \mathcal{L}^{(6)}, \tag{1}$$

where μ is the quark chemical potential, and m_q is the current quark mass. The four-quark interaction $\mathcal{L}^{(4)}$ consists of $\mathcal{L}^{(4)}_{\chi}$ and $\mathcal{L}^{(4)}_{s}$, which correspond to the qq and $q\bar{q}$ channel respectively. The six-quark interaction $\mathcal{L}^{(6)}$ describes the chiral-diquark interplay, which consists of two parts $\mathcal{L}^{(6)}_{\chi}$ and $\mathcal{L}^{(6)}_{\chi s}$. The chiral condensate is defined as

$$\chi\delta_{ij} = \langle\bar{q}_i q_j\rangle, \tag{2}$$

where the indices (i, j) are flavor of quark. For three-color and three-flavor QCD, the diquark condensate is defined as [20]

$$s_{AA'} = \langle q^T C\gamma_5\tau_A\lambda_{A'}q\rangle, \tag{3}$$

where τ_A and $\lambda_{A'}$ denote three antisymmetric Gell-Mann matrices, i.e., $A = 2, 5, 7$. If we neglect the current quark mass, dense matter is expected to form a so-called color-flavor-locked matter, characterized by the unique diquark condensate $s = s_{22} = s_{55} = s_{77}$.

In the mean-field approximation, the interaction terms in Lagrangian can be written as[7],

$$\mathcal{L}^{(4)}_{\chi} = 4G\chi\bar{q}q - 6G\chi^2, \tag{4}$$

$$\mathcal{L}^{(4)}_{s} = H[s^*(q^T C\gamma_5\tau_A\lambda_A q) + h.c.] - 3H|s|^2, \tag{5}$$

$$\mathcal{L}^{(6)}_{\chi} = -2K\chi^2\bar{q}q + 4K\chi^3, \tag{6}$$

$$\mathcal{L}^{(6)}_{\chi s} = -\frac{K'}{4}|s|^2\bar{q}q - \frac{K'}{4}\chi[s^*(q^T C\gamma_5\tau_A\lambda_A q) + h.c.] + \frac{3K'}{2}|s|^2\chi. \tag{7}$$

In the four-quark interaction, the couplings for qq-channel and $q\bar{q}$-channel are G and H respectively. $\mathcal{L}^{(6)}_{\chi}$ is the standard Kobayashi-Maskawa-'t Hooft interaction which couples the chiral condensate only, and the interaction coupling is written as K. For the six-quark term $\mathcal{L}^{(6)}_{\chi s}$ with coupling K', it corresponds to the interplay between chiral and diquark condensates.

Based on the equations above, all the $q\bar{q}$-channel interaction terms can be attributed as the constituent quark mass (the dynamic Dirac mass)

$$M = -4(G - \frac{1}{8}K\chi)\chi + \frac{1}{4}K's^2. \tag{8}$$

all可以去掉

We ignore the current quark mass m_q all through this work. The constituent mass is not only made up by four-quark interaction with G, but also related to the axial anomaly, manifesting as the Kobayashi-Maskawa-'t Hooft interaction of six-quark interaction K and the chiral-diquark interplay K'.

Similarly, the qq-channel interaction can be given as the color-superconductor gap (the dynamic Majorana mass)

$$\Delta = -2Hs + \frac{1}{2}K'\chi s. \tag{9}$$

The coupling H represents the magnitude of diquark attractive interaction. When the axial anomaly is introduced, it becomes

$$H' = H - \frac{1}{4}K'\chi. \tag{10}$$

The additional chiral-diquark interplay K' enhances the diquark attraction. This is the reason that the axial anomaly raises the COE of $\langle\bar{q}q\rangle$, $\langle qq\rangle$ and the diquark BEC phase. So that the diquark gap is given as $\Delta = -2H's$.

It is well known that the coupling H represents the magnitude of diquark attractive interaction. Its appropriate value makes color superconducting becomes possible. If the axial anomaly is introduced, the effective coupling becomes Eq. (10). Therefore, the additional chiral-diquark interplay enhance the diquark coupling. This is the essential reason that the axial anomaly raise the COE of chiral and diquark condensates and thus diquark BEC phase occur. We will investigate this effective coupling with magnetic field in the later section.

In the absence of magnetic field, the thermodynamic potential is written as

$$\Omega = \Omega_q + U(\chi, s). \tag{11}$$

By using the Nambu-Gor'kov formalism, the one-loop contribution given as[7],

$$\Omega_q = -8\sum_{\pm}\int\frac{d^3p}{(2\pi)^3}|\epsilon^8| - \sum_{\pm}\int\frac{d^3p}{(2\pi)^3}|\epsilon^1|, \tag{12}$$

where the sum indices $\pm$ represent the quasiparticle and anti-quasiparticle excitations respectively. In reference[7], the renormalization parameter Λ is cut-off for integral. The dispersion relation in singlet and octet representations read

$$\epsilon^1 = \sqrt{(E \pm \mu)^2 + (2\Delta)^2}, \quad \epsilon^8 = \sqrt{(E \pm \mu)^2 + \Delta^2}, \tag{13}$$

with the single-particle energy $E = \sqrt{p^2 + M^2}$.

The interaction potential U can be derived from Eqs.(4 -7), which reads[7]

$$U(\chi, s) = 6G\chi^2 - 4K\chi^3 + 3(H - \frac{K'}{2}\chi)s^2. \tag{14}$$

B. Formalism in the presence of magnetic field

When the magnetic field is introduced in the CFL matter, the most important physics is the rotated-electromagnetic mechanism[4], namely the rotated magnetic field make up by the linear combination of an usual photon and the eighth gluon fields. This unbroken symmetry is described by the subgroup $U(1)_{\widetilde{Q}}$, with $\widetilde{Q} = Q \times \mathbf{1} + \mathbf{1} \times T_8/\sqrt{3}$, where the electromagnetic charge operator $Q = \mathrm{diag}(-\frac{1}{3}, -\frac{1}{3}, \frac{2}{3})$ for (s, d, u) and the 8th Gell-Mann matrix $T_8 = \mathrm{diag}(-\frac{1}{\sqrt{3}}, -\frac{1}{\sqrt{3}}, \frac{2}{\sqrt{3}})$ for (b, g, r). The ansatz of the magnetic color-flavor-lock matter reads

$$s = s_{22}, \quad s_B = s_{55} = s_{77}. \tag{15}$$

In principle, the resulting condensates involve the color-antitriplet, flavor-antitriplet channel and color-sextet, flavor-sextet channel[17]. As discussed in literature[16], the sextet channel is usually ignored. According to the $\widetilde{Q}$ properties of quarks, there actually exist three types of pairing patterns: the neutral, charged and mixed pairings as summarized in Table I[15].

TABLE I: classification of pairings, gaps and dispersion relations

Paring type	neutral	mixed	charged
Quark	bd gs	ru gd bs	rs bu gu rd
$\widetilde{Q}$	0 0	0 0 0	+1 -1 -1 +1
Diquark condensate	s	s s_B	s_B
Gap	Δ	Δ_1, Δ_2	Δ_B
Dispersion relation	ϵ^n	$\epsilon_1^m, \epsilon_2^m$	ϵ^c

For the neutral type ($bd-gs$ pairing), only the diquark condensate s is involved and the color superconductor gap is determined by it. In the NJL-model with axial anomaly, the gap reads

$$\Delta = -2H's. \tag{16}$$

Correspondingly, the dispersion relation has the form like

$$\epsilon^n = \sqrt{(E \pm \mu)^2 + \Delta^2}, \tag{17}$$

for the quark and anti-quark excitations respectively. In Eq.(17), the single particle energy is still $E = \sqrt{p^2 + M^2}$, although the quark mass in Eq. (8) needs to be modified(see below). The neutral pairing contributes one-loop thermodynamic potential

$$\Omega_q^n = -6 \sum_{\pm} \int h_\Lambda \frac{d^3p}{(2\pi)^3} |\epsilon^n|, \tag{18}$$

where the smooth regulator function h_Λ has replaced the cut-off regulator scheme in Eq.(12).

For the charged type, the paired quarks carry the non-zero rotated charges (the $rs - bu$ and/or $gu - rd$ pairing, see Table I). The gap is determined by the diquark condensate s_B,

$$\Delta_B = -2H' s_B. \tag{19}$$

In this case, the single -particle energy spectrum becomes

$$E_B = \sqrt{p_3^2 + M^2 + 2neB}, \tag{20}$$

where p_3 is the third component of momentum space, and n is Landau level index($n = 0, 1, 2, ...$). The dispersion relations reads

$$\epsilon^c = \sqrt{(E_B \pm \mu)^2 + \Delta_B^2}, \tag{21}$$

where the gap $\Delta_B = -2H' s_B$. By using the substitution:

$$2 \int \frac{d^3p}{(2\pi)^3} \to \frac{eB}{8\pi^2} \sum_n^\infty (2 - \delta_{n0}) \int_{-\infty}^{+\infty} dp_3, \tag{22}$$

one can derive the thermodynamic potential contribution from charged quarks. For the given cut-off parameter Λ, we introduce the number of completely occupied Landau levels n_{max},

$$n_{max} = \mathrm{Int}[\frac{\Lambda^2}{2eB}], \tag{23}$$

and obtain the one-loop thermodynamic potential

$$\Omega_q^c = -8 \sum_{\pm} \frac{eB}{8\pi^2} \sum_{n=0}^{n_{max}} (2 - \delta_{n0}) \int h_{\Lambda,B}^n dp_3 |\epsilon^c|, \tag{24}$$

where $h_{\Lambda,B}^n$ is smooth regularization function for the charged pairing. Together with h_Λ , they will be discussed in the following section.

For the mixed type(i.e. $ru - gd - bs$ pairing), both s and s_B play their roles. As detailed in Ref.[17, 21], the color-superconductor gaps behave as the combination of Δ and Δ_B,

$$\Delta_1 = \frac{1}{2}(\sqrt{\Delta^2 + 8\Delta_B^2} + \Delta), \quad \Delta_2 = \frac{1}{2}(\sqrt{\Delta^2 + 8\Delta_B^2} - \Delta). \tag{25}$$

And the dispersion relation given as

$$\epsilon_1^m = \sqrt{(E \pm \mu)^2 + \Delta_1}, \quad \epsilon_2^m = \sqrt{(E \pm \mu)^2 + \Delta_2} \tag{26}$$

Since only neutral quarks are included in the mixed pairing, the thermodynamic potential contribution reads [21]

$$\Omega_q^m = -2\sum_{\pm} \int h_\Lambda \frac{d^3p}{(2\pi)^3}\epsilon_1^m - 2\sum_{\pm} \int h_\Lambda \frac{d^3p}{(2\pi)^3}\epsilon_2^m. \tag{27}$$

Now we turn to investigate the constituent mass in the magnetized CFL matter. Recalling that it stems the interacting terms in the $\bar{q}q$ channel, which is irrelevant to qq channel. M has the similar form as Eq.(8), as long as the splitting of diquark condensate is taken into account. While the first term in R.H.S. of Eq.(8) holds unchanged, the splitting changes the second term of Eq.(8) through the chiral-diquark coupling K'. Due to a simple relation $s_{22}^2 + s_{55}^2 + s_{77}^2 = s^2 + 2s_B^2$, the zero-field result s^2 should be replaced $\frac{1}{3}s^2 + \frac{2}{3}s_B^2$ in the presence of magnetic field. Thus Eq.(8) in the zero-field result is rewritten as

$$M = -4(G - \frac{1}{8}K\chi)\chi + \frac{1}{12}K's^2 + \frac{1}{6}K's_B^2, \tag{28}$$

The constituent quark mass can be derived form the Nambu-Gor'kov formalism, and then contribution term of the constituent quark mass comes form the diagonal of the inverse propagator, while the off-diagonal term effect the quark splitting[7]. Thus thus the gap splitting have no influence to the formalism of constituent quark mass. Following the same procedure, the interaction potential term Eq. (14) is given by

$$U(\chi, s, s_B) = 6G\chi^2 - 4K\chi^3 + (H - \frac{K'}{2}\chi)(s^2 + 2s_B^2). \tag{29}$$

Instead of Eq. (11), the total thermodynamic potential is the function of

$$\Omega(\chi, s, s_B) = \Omega_q^n + \Omega_q^m + \Omega_q^c + U. \tag{30}$$

In Eq. (30), the contribution from electromagnetic field (say, $\frac{1}{2}B^2$) in this equation has been dropped out, since the magnetic filed penetrate the CFL quark matter freely [15, 17, 18].

C. Regularization scheme and Model parameters

In the case of non-zero magnetic field, it is well known that the hard cutoff scheme is not suitable. In literature, Several smooth renormalization scheme have been considered. For

instance, the smooth regularization functions, e.g. Gaussian-function$\sim exp(-p^2/\Lambda^2)$[21], Lorentzian-function$\sim [1+(\frac{p}{\Lambda})^N]^{-1}$[22], as well as Wood-Saxon-function[23] have been introduced. In our work we follow the Lorentzian-function, so that the smooth regularization factor given in eqs. (18), (24) and (27) reads

$$h_\Lambda = [1+(\frac{p}{\Lambda})^N]^{-1}, h^n_{\Lambda,B} = [1+(\frac{\sqrt{p_3^2+2neB}}{\Lambda})^N]^{-1} \tag{31}$$

respectively. N is the index of the smooth regularization factor and n is Landau levels number. The numerical calculation shows that $N=5$ in Eq.(31) is appropriate to improve the unphysical oscillation.

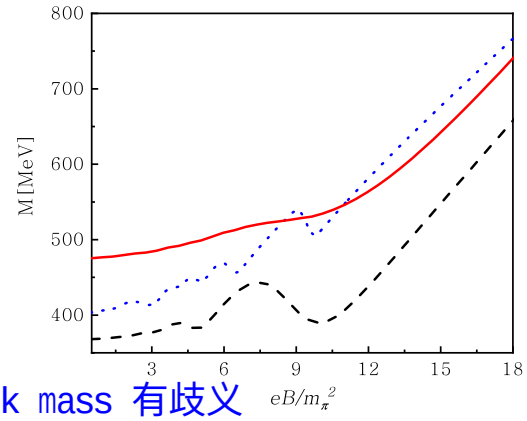

FIG. 1: Quark mass for low chemical potential with Lorentzian-function with $N=5$ (red solid line) and $N=15$ (black dashed-line) and Gaussian-type (blue dotted line).

As for the model parameter G, H, K', K and Λ, the regulation parameter Λ and the chiral coupling constant G is fixed by fitting the pion properties in vacuum, e.g., the pion mass $m_\pi = 140$MeV and the constituent quark mass $M = 340$MeV. The diquark coupling constant H is fixed by fitting the scalar diquark gaps. For the six-fermion coupling constants K and K', one appropriate value of $K'/K = 4.2$[7] which satisfy the appearance of low-temperature critical phenomena. In the present work, we adopt the parameters of Table I ($m_q = 0$) in Ref.[7].

III. NUMERICAL CALCULATIONS AND DISCUSSIONS

The phase structure can be determined, through self-consistent calculation, by looking for the global minimum of thermodynamic potential in Eq. (30) with respect to three order parameter s, s_B and χ. Then, the gap equations can be derived from

$$\frac{\partial\Omega}{\partial s}=0,\quad \frac{\partial\Omega}{\partial s_B}=0,\quad \frac{\partial\Omega}{\partial\chi}=0. \tag{32}$$

Before studying the phase diagram, we need to define the different Bose-Einstein condensed phases of diquark condensate. The condensed phase with $s_B\neq 0$ and $s=0$ is refered as $\mathrm{BEC_I}$ phase in the present work. And the condensed phase with $s_B=0, s\neq 0$ is refered as $\mathrm{BEC_{II}}$ phase. Besides, the phase with nonzero s and s_B corresponds to an ordinary BEC phase.

A. COE phase region and critical phenomena

By using the given model parameters, we calculate COE phase at a weak magnetic field. As a typical result displayed in Fig.2, magnetic field obtained at $eB=4.6m_\pi^2$. When the quark chemical potential $\mu=\mu_c^I=313$MeV, the $\mathrm{BEC_I}$ phase occurs (μ_c^I denotes the critical value of $\mathrm{BEC_I}$ occurrence thereafter). As μ increases to almost 327MeV, the BEC phase occurs. At $\mu=\mu_X\approx 350$MeV, the crossover between BEC and BCS appear, since the reference chemical point μ_X is determined by the condition $M=\mu$ (see, e.g. [24]).

The result of Fig.2 is basically same to the zero-field result. As the zero-field case, the COE region and critical phenomena still exist. The difference is that the new $\mathrm{BEC_I}$ phase preceded the BEC phase to appears in the COE region. (change this sentence to "The difference is that the BEC_I phase, preceding the BEC, is newly appearing in COE region.") Also, the value of quark mass obtained in Fig.2 is usually large than that given by Ref.[7], which is associated with our used smooth regularization partly.

With increasing magnetic filed, COE phase structure and critical phenomena will have remarkable change. Numerical result shows that the $\mathrm{BEC_I}$ phase gradually occupies the whole COE region. In other words, the BEC phase is suppressed by the strong magnetic field. As BEC comes to be removed form the phase diagram, the magnetic field corresponds to a threshold value, which will be discussed below.

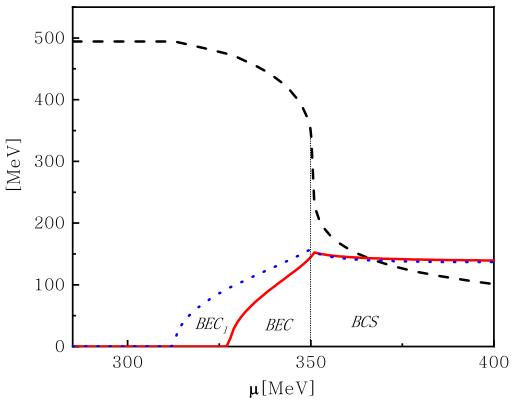

FIG. 2: Constituent quark mass M(dashed-line), and color-superconductor gaps for diquark condensate Δ(red solid line) and Δ_B(blue dotted line) as functions of μ under magnetic field value $eB/m_\pi^2 = 4.6$.

In Fig.3, we give a typical result of strong magnetic field, $eB = 9.2m_\pi^2$. When $\mu = \mu_c^I$, the constituent quark mass M still have continuity, while the Δ_B start to appear. However, at the reference point $\mu_X = 338$MeV, the continuity of three gaps (especially M) is destroyed. It indicates that a second order transition predicted in zero-field case turns into a first order transition. In other words, the previously predicted critical phenomena at μ_X no longer exists . Also, the calculation shows that this conclusion holds unchanged , unless the chiral-diquark coupling K' is chosen too large.

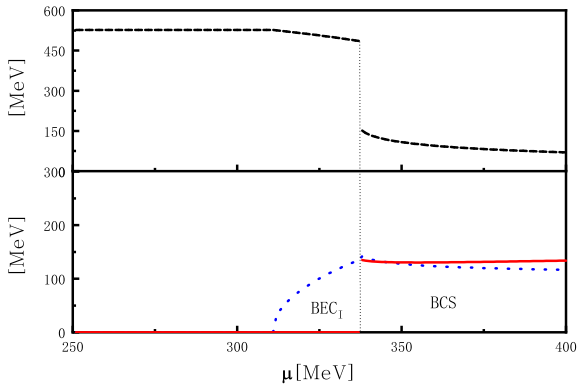

FIG. 3: Similar as Fig.2, but for magnetic filed eB/m_π^2 equals to 9.2.

B. Critical chemical potentials for different BEC occurrences

In order to better understand the phase structure obtained in Sec.III A, our attention is focused on the criteria of diquark Bose-Einstein condensed phases. As a second-order transition, occurrence of a designated BEC phase can be determined by the Thouless criterion[25], i.e.,

$$\frac{1}{H'} = Q(\vec{q}=0,\omega=0), \tag{33}$$

where H' is effective diquark coupling , and $Q(\vec{q},\omega)$ is diquark polarization function deriving from the usual quark propagator at one-loop level[25]. In the absence of magnetic field, the polarization function is easily obtained and the BEC occurrence is determined by [7]

$$\frac{1}{4H'} = 4\sum_{\pm}\int \frac{d^3p}{(2\pi)^3}\frac{1-2f(E\pm\mu)}{2(E\pm\mu)}dp, \tag{34}$$

with $E=\sqrt{p^2+M^2}$ and $f(\epsilon)=1/(e^{\epsilon/T}+1)$ is the Fermi distribution function. At zero temperature, Eq. (34) has the form

$$\frac{1}{H'} = \frac{8}{\pi^2}\int_0^{\Lambda}\frac{Ep^2}{E^2-\mu^2}dp, \tag{35}$$

where E is the single-particle energy and the hard cut off regulator scheme is included.

Let's firstly consider the criterion of $\mathrm{BEC_{II}}$. $\mathrm{BEC_{II}}$ involved order parameter is s and the paired quarks involved in s are always neutral. Thus there is no direct coupling to magnetic field. Similar to Eq. (35), the criterion of $\mathrm{BEC_{II}}$ can be derived as

$$\frac{1}{H'} = \frac{8}{\pi^2}\int h_\Lambda\frac{Ep^2}{E^2-\mu^2}dp, \tag{36}$$

the smooth regulator function h_Λ is introduced in the presence of magnetic field.

For $\mathrm{BEC_I}$, the involved order parameter is s_B. As shown in Table.I, the paired quarks consist of two classes: neutral quarks and rotated-charged quarks. For the rotated charge quarks, the necessary substitution should be made. By taking into account the contributions from both charged and neutral quarks, then the criterion of $\mathrm{BEC_I}$ becomes

$$\frac{1}{H'} = \frac{eB}{2\pi^2}\int\sum_{n=0}^{n_{max}}(1-\frac{\delta_{n0}}{2})h^n_{\Lambda,B}\frac{E_B}{E_B^2-\mu^2}dp_3 + \frac{4}{\pi^2}\int h_\Lambda\frac{Ep^2}{E^2-\mu^2}dp. \tag{37}$$

In the first term of R.H.S, the explicit coupling to eB has been introduced by the Landau level. In zero-field limit, the form of Eq. (37) is recovered to the known result Eq. (36).

Also, the criteria can be derived in the alternative way. Regarding the thermodynamic potential, the criteria of $\mathrm{BEC_I}$ and $\mathrm{BEC_{II}}$ can be described by a Ginzburg-Landau expansion of Δ and Δ_B. As the second order transition, the criteria are given by the vanishing Ginzburg-Landau coefficient of quadratic term, i.e.,

$$\frac{\partial^2\Omega}{\partial\Delta^2}|_{\Delta_B=0,\Delta=0}=0,\frac{\partial^2\Omega}{\partial\Delta_B^2}|_{\Delta_B=0,\Delta=0}=0. \tag{38}$$

It is easily proven that the above result are consistent with Eqs. (36) and (37).

FIG. 4: Critical values μ_c^{I} (red solid line), μ_c^{II} (green dashed line) and μ_c for BEC (blue dashed dotted line) vs. the reference chemical potential μ_X (black dotted line)

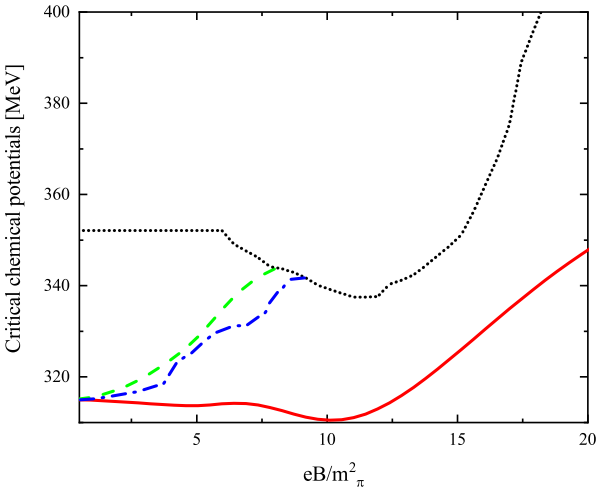

By using Eqs. (36) and (37), we calculate the critical values for Bose-Einstein Condensed phases with the given model parameters. As shown in Fig.4, magnetic fields make the occurrences of various Bose-Einstein Condensed phases separated. Firstly, it is clear that with introducing B, μ_c^{I} comes to be smaller than μ_c^{II}, which means the $\mathrm{BEC_I}$ phase occurs firstly. If $\mathrm{BEC_{II}}$ exists, it would have the position for $eB \lesssim 8m_\pi^2$. In such a regime, there actually is $\mathrm{BEC_I}$ and/or BEC rather than $\mathrm{BEC_{II}}$, which has been observed in figs. 2 and 3. Secondly, as shown in Fig.3, the BEC phase appears only for intermediate magnetic field. It is shown in Fig.4 that the BEC existence remains valid until $eB \approx 9m_\pi^2$ at which the line of μ_c meets the line of μ_X. The magnetic field $eB \approx 9m_\pi^2$ corresponds to the threshold value of magnetic field mentioned above. For the magnetic field whose value is larger than the threshold value, μ_c^{I} is always less than μ_X. So that the $\mathrm{BEC_I}$ exists throughout the remaining regime.

Moreover, it is worthy being stressed that the various of critical chemical potentials have the different magnetic-field-dependence. For $\mathrm{BEC_{II}}$ and BEC, the critical values are almost monotonic increasing functions. However, μ_c^{I} is not a increasing function, at least at $6m_\pi^2 < eB < 10m_\pi^2$ regime. It is noticed that critical phenomena appears at μ_c^{I} and μ_c^{I} can be understood as the critical end point of chiral phase transition, Therefore the decreasing tendency of μ_c^{I} means that chiral phase transition occur at relatively low chemical potential with increasing magnetic field. Such of phenomenon contradicts with the known magnetic [12, 13]. It may be regarded as inverse magnetic catalysis. To this end, one may wonder whether or not the IMC effect originate from the oscillation for three gaps. The possible oscillation is not the key reason that μ_c^{I} decreases in intermediate magnetic field. Even though nonphysical oscillation is removed, the conclusion of IMC can still be drawn, as stressed in Ref.[26].

C. Strong field analysis for $\mathrm{BEC_I}$ occurrence

In the strong field limit, the lowest Landau level works and the system dimension could be reduced to $1+1$ dimension. In literatures, the situation with strong magnetic field has been widely discussed. For the pure chiral-broken phase (the phase with $\chi \neq 0$ only), the magnetic effect becomes important as long as $eB \sim m_\pi^2$. As a typical example, the strong fields in heavy ion collision experiments are observed to have magnitudes of the order $eB \approx 15m_\pi^2$[27]. For the pure BCS phase of magnetized CFL matter (the phase with diquark condensates only), the relevant scale for the generation of the diquark gaps is the quark chemical potential. Once the magnitude of the magnetic field is comparable to the chemical potential, i.e. $eB \sim \mu^2$, as pointed in [15], the density of states on the Fermi surface of the charged quarks will be larger than that of neutral quarks. In the context regarding COE consisted of chiral and diquark condensate, our concerned quark matter region is determined by $M = \mu$. In this sense strong field means that $eB \sim \mu^2 = M^2$.

For $\mathrm{BEC_I}$ occurrence, its criterion Eq.(37) may be simplified in strong field limit. The first term of R.H.S. in Eq. (37) becomes

$$\frac{eB}{2\pi^2}\int h_{\Lambda,B}^{n=0}\frac{\sqrt{p_3^2+M^2}}{p_3^2+M^2-\mu^2}dp_3. \tag{39}$$

And Eq. (37) can be simplified as

$$\frac{1}{H'}=\frac{eB}{2\pi^2}\int_0^{\Lambda}\frac{E}{E^2-\mu^2}dp+\frac{4}{\pi^2}\int_0^{\Lambda}\frac{E}{E^2-\mu^2}p^2dp, \tag{40}$$

Note that, in the strong field limit, the single-particle energy reduces to $E=\sqrt{p^2+M^2}$ and one may adopt the hard cutoff regularization scheme. Obviously, Eq. (40) could give the result of Fig.4 for $\mathrm{BEC_I}$ in the strong field regime. Compared with Fig.4, Eq. (40) becomes valid for $eB\gtrsim 11m_\pi^2$, which is the strong field regimes in our numerical calculations.

FIG. 5: Solid line denotes ratio of the effective coupling required for $\mathrm{BEC_I}$ in strong field limit. Dashed line has ignored the magnetic effect from M.

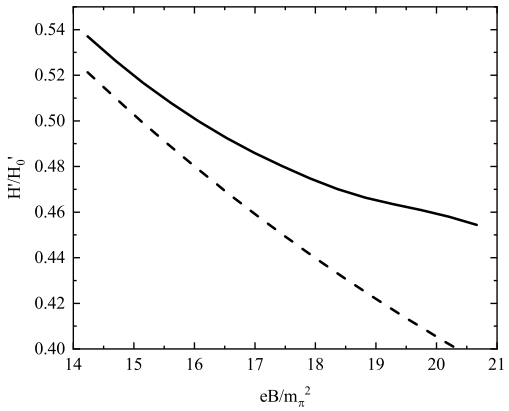

In the absence of magnetic fields, as stressed in Ref.[7], the axial anomaly leads to the chiral-diquark interplay K' and makes the diquark coupling become effective $H'=H-\frac{1}{4}K'\chi$. We will apply Eq. (40) to investigate how the coupling H' varies with the strong fields. In Fig.5, we give the magnetic-field dependence of H' at a given quark chemical potential ($\mu=315\mathrm{MeV}$). Note that we have normalized the diquark effective coupling H' with respect to the value H'_0 obtained in the $B=0$ situation. As depicted in Fig.5, the solid line manifests a monotonic decreasing function. It indicates that a relatively small H' could make $\mathrm{BEC_I}$ occur in strong field regime. In other words, strong fields facilitate the occurrence of $\mathrm{BEC_I}$. This tendency mainly originates from an explicit coupling to eB (i.e., the first term of Eq. (40)). Besides, the strong field result of H' orignates from an implicit B-dependence of E, exactly the dependence of quark mass. Interestingly, the B-dependence of quark mass displays a monotonic increasing function (magnetic catalysis for strong fields regime [12, 13]). If neglecting this kind of dependence of M, H' as a function of eB would be a more

obvious decreasing function as shown by dashed line. It is clear in Fig.5 that the magnetic effect caused by the eB coupling is partial compensated that the magnetic effect from M.

FIG. 6: Phase diagram in the μ-K' plane. Thick (red) solid line denotes the first-order phase transition, thin (green) solid line $\mathrm{BEC_I}$ transition and dotted (blue) line BEC-BCS crossover.

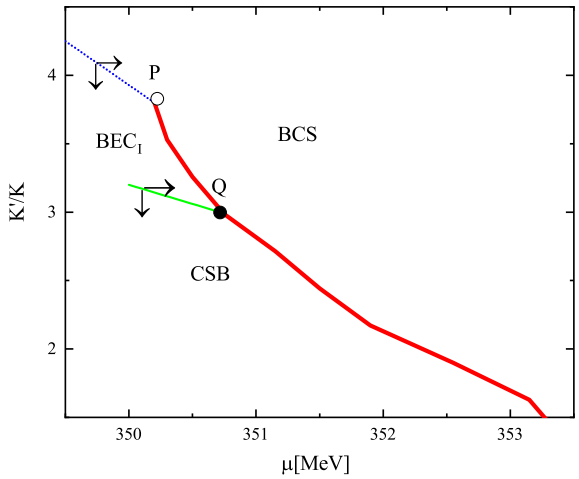

Now let us turn to focus on the chiral-diquark interplay K' variations. In Fig.6, the phase diagram in the μ-K' plane is plotted. For small K', the phase diagram has a chiral symmetry broken (CSB) region and a BCS region, separated by the first-order phase transition line, shown as thick solid line. As K' obtains the required value for Eq.(40), $\mathrm{BEC_I}$ appears across a second-order phase transition from the CSB phase, shown as thin solid line. With increasing K', $\mathrm{BEC_I}$ will undergo a crossover to the BCS phase, shown as dotted line. In Fig.6, there exist two intersections: the thin solid line meets the thick solid line at point Q and the dotted line meets the thick solid line at point P. The point Q is a critical end point of chiral transition , since the order parameter M is continuous. As for the point P, it could not be regarded as a critical end point. Therefore, in Fig.3, the order parameter M is discontinuous and critical phenomenon does not appear.

Finally, let us discuss the B-dependent evolution of $\mathrm{BEC_I}$ phase in K'-μ phase diagram qualitatively. In a given strength of K', the thin solid line and dotted line shift to larger chemical potentials with increasing magnetic field. This tendencies are shown by the horizontal arrows in Fig.6. It indicates that strong fields make the location of $\mathrm{BEC_I}$ moves towards higher densities in phase diagram.

In the situation of given chemical potentials, on the other hand, the thin solid line and dotted line move towards a lower K'. This tendencies are shown by the vertical arrows in Fig.6. It indicates that the existence of strong fields makes chiral-diquark interplay required become weaker. It is qualitative consistent with the results of H' shown in Fig.5. Because it requires smaller strengths of QCD axial anomaly with increasing magnetic field.

IV. CONCLUSION AND OUTLOOK

In this work we investigate coexistence of chiral and diquark condensates and moderate-density and zero-temperature critical phenomenon in the presence of magnetic fields. Generally, critical phenomena depend on the symmetries and symmetry breaking patterns of order parameters. In the absence of magnetic fields, the model-independent analyses had been given for the critical phenomenon [5, 6]. The CFL breaking pattern is $SU(3)_C \times SU(3)_L \times SU(3)_R \times U(1)_B \times U(1)_A \to SU(3)_{C+L+R}$. Within a Ginzburg-Landau (GL) framework, diquark condensate can be described by a 3×3 matrix, say $d_L = -d_R = \mathrm{diag}(s, s, s)$ in the chiral limit. Similarly, chiral condensate is described by the matrix $\Phi = \mathrm{diag}(\chi, \chi, \chi)$. As stressed in Ref.[6], the axial anomaly yields cubic terms, especially the term like $s^2\chi$, in the GL free energy and the chiral-diquark interplay leads to the critical phenomenon in the phase diagram. Once strong magnetic fields are introduced, the symmetry is further broken to $SU(2)_{C+L+R}$[17] and the magnetized CFL matter appears at high densities. A similar GL analysis is valid at least for the COE phase with non-vanishing s_B and χ. While the matrix Φ holds unchanged, diquark condensate becomes $d_L = -d_R = \mathrm{diag}(0, s_B, s_B)$. In this case, there exists such GL term as $s_B^2\chi$ and thus a magnetic field does not preclude the axial-anomaly induced critical phenomenon. From our results, for instance, the point Q in Fig.6 corresponds to the critical end point of chiral transition and the critical phenomenon still takes place around it. On the other hand, it is difficult to proceed the GL analysis for the situation with non-zero s, s_B and χ. Due to the magnetic-induced splitting, the diquark-condensate matrix decomposes into two parts, namely the part relevant to $\frac{1}{3}(s + 2s_B)$ and that relevant to $\mathrm{diag}(\frac{2}{3}, -\frac{1}{3}, -\frac{1}{3})$. Now that electric charge matrix emerges in the latter, the electromagnetic field needs to be incorporated into the GL free energy. Also, the possible rotation between d_L and d_R need to be considered. A qualitative GL analysis could not explain the COE phase and the associated

critical phenomena, unless these microscopic details are known.

The quantitative discussions of magnetic influences on COE and critical phenomenon are the main content of the present work. In a phenomenological NJL model with axial anomaly, we derive the formalism of magnetized CFL matter and the criteria of different Bose-Einstein Condensed phases. Besides the complicated COE phase structure, our attention is mainly paid to the $\mathrm{BEC_I}$ occurrence. For various strengths of magnetic field, we briefly discuss several implications of the main results.

(i) The inverse magnetic catalysis (IMC) is observed for intermediate fields, say $6m_\pi^2 < eB < 10m_\pi^2$ according to our numerical calculations. This phenomenon has been widely predicted from the high-temperature Lattice QCD to the model studies in zero temperature case [11, 26]. In two-color and two-flavor NJL model without axial anomaly, the quarks with rotated electric charges $\pm\frac{1}{2}$ were considered in Ref.[26]. As the COE phase, the resulting Bose-Einstein Condensed phase is similar as the present-discussed $\mathrm{BEC_I}$. It is not surprising then that our result of IMC has analogy to the case of Ref.[26].

(ii) The role of strong fields that facilitate the $\mathrm{BEC_I}$ occurrence is clarified by arguments in the lowest Landau-level limit. For the fields $eB > 11m_\pi^2$, its critical value μ_c^I is observed to increase monotonically. Stronger fields mean that $\mathrm{BEC_I}$ (as the COE phase) is located at larger quark chemical potentials and/or higher baryon densities. At the same time, it requires smaller strengths of the chiral-diquark coupling K' and/or smaller strengths of the effective coupling H'. Note that the QCD axial anomaly is believed to become suppressed in high-density quark matter, see,e.g. [28, 29]. By introducing strong fields, therefore, $\mathrm{BEC_I}$ and the COE phase region are updated to exist in more realistic situation and/or more reasonable physical environment.

This theoretical prediction could have potentially importance for astrophysics, since $eB \simeq 11m_\pi^2 \sim 10^{20}\mathrm{G}$ discussed here reaches the estimated value for interior field in magnetars [19]. Taking the BCS phase of magnetized CFL matter into account, stellar models of hybrid stars with quark core and self-bound quark stars had been studied in recent years, see, e.g. Refs.[30, 31]. If $\mathrm{BEC_I}$ exists and constitutes the interiors, it is likely that stellar models of mixed stars with the core of COE (without sharp interface) would be needed. Also, such kind of possibility might represent a new open

opportunity for exploring the the continuity between chiral-broken matter and color superconducting matter.

The present study is based on a minimal extension of the NJL model with axial anomaly. In more realistic NJL models where multiple flavors with bare masses, effect of confinement, color neutrality and so on are considered, the resultant phase structure becomes more and more complicated unavoidably, see, e.g. [8, 9, 32]. In the presence of magnetic fields, not merely splitting of diquark condensate but also "splitting" of the longitudinal and transverse pressures are important for applications of CFL matter. The latter was taken into account in Ref.[31], but has not been considered in the present work. Also, there are alternative smooth regularization schemes in the studies of magnetized matter with diquark condensate. For instance, the scheme called magnetic field independent regularization was adopted to remove nonphysical oscillations of gaps [26, 33]. Towards further studies of our presented $\mathrm{BEC_I}$ and its applications inside magnetars, we will discuss these problems listed above in a future publication.

---

[1] F. Wilczek M. Alford, K. Rajagopal. Color-flavor locking and chiral symmetry breaking in high density qcd. *Nucl. Phys. B.*, 537:443, 1999.

[2] Mark Alford. Dense quark matter in nature. *Prog. Theor. Phys. Suppl.*, 153:1–14, 2004. doi: 10.1143/PTPS.153.1.

[3] Mark G. Alford, Andreas Schmitt, Krishna Rajagopal, and Thomas Schäfer. Color superconductivity in dense quark matter. *Rev. Mod. Phys.*, 80:1455–1515, Nov 2008. doi: 10.1103/RevModPhys.80.1455. URL https://link.aps.org/doi/10.1103/RevModPhys.80.1455.

[4] Mark G. Alford, Krishna Rajagopal, and Frank Wilczek. QCD at finite baryon density: Nucleon droplets and color superconductivity. *Phys. Lett.*, B422:247–256, 1998. doi: 10.1016/S0370-2693(98)00051-3.

[5] Naoki Yamamoto, Motoi Tachibana, Tetsuo Hatsuda, and Gordon Baym. Phase structure, collective modes, and the axial anomaly in dense qcd. *Phys. Rev. D*, 76:074001, Oct 2007. doi: 10.1103/PhysRevD.76.074001. URL https://link.aps.org/doi/10.1103/PhysRevD.76.074001.

[6] Tetsuo Hatsuda, Motoi Tachibana, Naoki Yamamoto, and Gordon Baym. New critical point

induced by the axial anomaly in dense qcd. *Phys. Rev. Lett.*, 97:122001, Sep 2006. doi: 10.1103/PhysRevLett.97.122001. URL https://link.aps.org/doi/10.1103/PhysRevLett.97.122001.

[7] Hiroaki Abuki, Gordon Baym, Tetsuo Hatsuda, and Naoki Yamamoto. Nambu–jona-lasinio model of dense three-flavor matter with axial anomaly: The low temperature critical point and bec-bcs diquark crossover. *Phys. Rev. D*, 81:125010, Jun 2010. doi: 10.1103/PhysRevD.81.125010. URL https://link.aps.org/doi/10.1103/PhysRevD.81.125010.

[8] H. Basler and M. Buballa. Role of two-flavor color superconductor pairing in a three-flavor nambu–jona-lasinio model with axial anomaly. *Phys. Rev. D*, 82:094004, Nov 2010. doi: 10.1103/PhysRevD.82.094004. URL https://link.aps.org/doi/10.1103/PhysRevD.82.094004.

[9] Philip D. Powell and Gordon Baym. Axial anomaly and the three-flavor nambu–jona-lasinio model with confinement: Constructing the qcd phase diagram. *Phys. Rev. D*, 85:074003, Apr 2012. doi: 10.1103/PhysRevD.85.074003. URL https://link.aps.org/doi/10.1103/PhysRevD.85.074003.

[10] Mikhail A. Stephanov. QCD phase diagram and the critical point. *Prog. Theor. Phys. Suppl.*, 153:139–156, 2004. doi: 10.1142/S0217751X05027965. [Int. J. Mod. Phys.A20,4387(2005)].

[11] Jens O. Andersen, William R. Naylor, and Anders Tranberg. Phase diagram of qcd in a magnetic field. *Rev. Mod. Phys.*, 88:025001, Apr 2016. doi: 10.1103/RevModPhys.88.025001. URL https://link.aps.org/doi/10.1103/RevModPhys.88.025001.

[12] V.P. Gusynin, V.A. Miransky, and I.A. Shovkovy. Dimensional reduction and dynamical chiral symmetry breaking by a magnetic field in 3 + 1 dimensions. *Physics Letters B*, 349(4):477 – 483, 1995. ISSN 0370-2693. doi: https://doi.org/10.1016/0370-2693(95)00232-A. URL http://www.sciencedirect.com/science/article/pii/037026939500232A.

[13] V. A. Miransky. Catalysis of dynamical symmetry breaking by a magnetic field. *Nucl. Phys. B*, 462(123):249290, 2012.

[14] Mark Alford, Jürgen Berges, and Krishna Rajagopal. Gapless color superconductivity. *Phys. Rev. Lett.*, 84:598–601, Jan 2000. doi: 10.1103/PhysRevLett.84.598. URL https://link.aps.org/doi/10.1103/PhysRevLett.84.598.

[15] Efrain J. Ferrer, Vivian de la Incera, and Cristina Manuel. Magnetic color-flavor locking phase in high-density qcd. *Phys. Rev. Lett.*, 95:152002, Oct 2005. doi: 10.1103/PhysRevLett.

95.152002. URL https://link.aps.org/doi/10.1103/PhysRevLett.95.152002.

[16] Kenji Fukushima and Harmen J. Warringa. Color superconducting matter in a magnetic field. *Phys. Rev. Lett.*, 100:032007, Jan 2008. doi: 10.1103/PhysRevLett.100.032007. URL https://link.aps.org/doi/10.1103/PhysRevLett.100.032007.

[17] Efrain J. Ferrer, Vivian de la Incera, and Cristina Manuel. Color-superconducting gap in the presence of a magnetic field. *Nucl. Phys.*, B747:88–112, 2006. doi: 10.1016/j.nuclphysb.2006.04.013.

[18] Efrain J. Ferrer and Vivian de la Incera. Magnetic phases in three-flavor color superconductivity. *Phys. Rev. D*, 76:045011, Aug 2007. doi: 10.1103/PhysRevD.76.045011. URL https://link.aps.org/doi/10.1103/PhysRevD.76.045011.

[19] Dong Lai and Stuart L Shapiro. Cold equation of state in a strong magnetic field-effects of inverse beta-decay. *Astrophys. J.*, 383:745–751, 1991.

[20] M. Buballa and M. Oertel. Colorflavor unlocking and phase diagram with self-consistently determined strange-quark masses. *Nuclear Physics A*, 703(3):770 – 784, 2002. ISSN 0375-9474. doi: https://doi.org/10.1016/S0375-9474(01)01674-8. URL http://www.sciencedirect.com/science/article/pii/S0375947401016748.

[21] Jorge L. Noronha and Igor A. Shovkovy. Color-flavor locked superconductor in a magnetic field. *Phys. Rev. D*, 76:105030, Nov 2007. doi: 10.1103/PhysRevD.76.105030. URL https://link.aps.org/doi/10.1103/PhysRevD.76.105030.

[22] Marco Frasca and Marco Ruggieri. Magnetic susceptibility of the quark condensate and polarization from chiral models. *Phys. Rev. D*, 83:094024, May 2011. doi: 10.1103/PhysRevD.83.094024. URL https://link.aps.org/doi/10.1103/PhysRevD.83.094024.

[23] Sh. Fayazbakhsh and N. Sadooghi. Color neutral two-flavor superconducting phase of cold and dense quark matter in the presence of constant magnetic fields. *Phys. Rev. D*, 82:045010, Aug 2010. doi: 10.1103/PhysRevD.82.045010. URL https://link.aps.org/doi/10.1103/PhysRevD.82.045010.

[24] Masakiyo Kitazawa, Dirk H. Rischke, and Igor A. Shovkovy. Bound diquarks and their boseeinstein condensation in strongly coupled quark matter. *Physics Letters B*, 663(3):228 – 233, 2008. ISSN 0370-2693. doi: https://doi.org/10.1016/j.physletb.2008.03.067. URL http://www.sciencedirect.com/science/article/pii/S0370269308003948.

[25] Yusuke Nishida and Hiroaki Abuki. Bcs-bec crossover in a relativistic superfluid and its

significance to quark matter. *Phys. Rev. D*, 72:096004, Nov 2005. doi: 10.1103/PhysRevD.72.096004. URL https://link.aps.org/doi/10.1103/PhysRevD.72.096004.

[26] Dyana C. Duarte, P. G. Allen, R. L. S. Farias, Pedro H. A. Manso, Rudnei O. Ramos, and N. N. Scoccola. Bec-bcs crossover in a cold and magnetized two color njl model. *Phys. Rev. D*, 93:025017, Jan 2016. doi: 10.1103/PhysRevD.93.025017. URL https://link.aps.org/doi/10.1103/PhysRevD.93.025017.

[27] V. Skokov, A. Yu. Illarionov, and V. Toneev. Estimate of the magnetic field strength in heavy-ion collisions. *Int. J. Mod. Phys.*, A24:5925–5932, 2009. doi: 10.1142/S0217751X09047570.

[28] T. Schäfer. Instanton effects in qcd at high baryon density. *Phys. Rev. D*, 65:094033, May 2002. doi: 10.1103/PhysRevD.65.094033. URL https://link.aps.org/doi/10.1103/PhysRevD.65.094033.

[29] R. Rapp, T. Schfer, E.V. Shuryak, and M. Velkovsky. High-density qcd and instantons. *Annals of Physics*, 280(1):35 – 99, 2000. ISSN 0003-4916. doi: https://doi.org/10.1006/aphy.1999.5991. URL http://www.sciencedirect.com/science/article/pii/S0003491699959912.

[30] Efrain J. Ferrer and Vivian de la Incera. Magnetism in Dense Quark Matter. *Lect. Notes Phys.*, 871:399–432, 2013. doi: 10.1007/978-3-642-37305-3_16.

[31] L. Paulucci, Efrain J. Ferrer, Vivian de la Incera, and J. E. Horvath. Equation of state for the magnetic-color-flavor-locked phase and its implications for compact star models. *Phys. Rev. D*, 83:043009, Feb 2011. doi: 10.1103/PhysRevD.83.043009. URL https://link.aps.org/doi/10.1103/PhysRevD.83.043009.

[32] Philip D. Powell and Gordon Baym. Asymmetric pairing of realistic mass quarks and color neutrality in the polyakov–nambu–jona-lasinio model of qcd. *Phys. Rev. D*, 88:014012, Jul 2013. doi: 10.1103/PhysRevD.88.014012. URL https://link.aps.org/doi/10.1103/PhysRevD.88.014012.

[33] M. Coppola, P. Allen, A. G. Grunfeld, and N. N. Scoccola. Magnetized color superconducting quark matter under compact star conditions: Phase structure within the $\mathrm{su}(2)_{\mathrm{f}}$ njl model. *Phys. Rev. D*, 96:056013, Sep 2017. doi: 10.1103/PhysRevD.96.056013. URL https://link.aps.org/doi/10.1103/PhysRevD.96.056013.